



# Seasonal variation and health risk assessment of atmospheric PM<sub>2.5</sub>-bound polycyclic aromatic hydrocarbons in a classic agglomeration industrial city, central China

Tianpeng Hu<sup>1,2</sup> · Jiaquan Zhang<sup>1</sup> · Xinli Xing<sup>2</sup> · Changlin Zhan<sup>1</sup> · Li Zhang<sup>1</sup> · Hongxia Liu<sup>1</sup> · Ting Liu<sup>1</sup> · Jingru Zheng<sup>1</sup> · Ruizhen Yao<sup>1</sup> · Junji Cao<sup>3</sup>

Received: 8 January 2018 / Accepted: 9 April 2018  
© Springer Science+Business Media B.V., part of Springer Nature 2018

## Abstract

Sixty atmospheric sample concentrations of PM<sub>2.5</sub> and polycyclic aromatic hydrocarbons (PAHs) in PM<sub>2.5</sub> were analyzed in distinct seasonal variations from a classic agglomeration industrial city. The concentrations of PM<sub>2.5</sub> ranged from 6.96 to 260.06 µg/m<sup>3</sup> with an average of 177.05 µg/m<sup>3</sup>. Only 38% of the sampling days were superior to the 24-h limit value (75 µg/m<sup>3</sup>) of ambient air quality standards (AAQs), and the samples from autumn and winter exceeded the limit value. The total PAHs ranged from 1.51 to 44.51 ng/m<sup>3</sup> with an average of 10.65 ng/m<sup>3</sup>. The highest and lowest concentrations of total PAHs appeared in winter and summer with averages of 22.56 and 4.03 ng/m<sup>3</sup>, respectively. Correlation analysis revealed that high-molecular-weight PAHs (HMW-PAHs) (4-, 5-, 6-ring PAHs) were significantly and negatively correlated with temperature and water-soluble total organic carbon (WTOC), and significantly correlated with water-soluble total nitrogen (WTN). The 4-, 5- and 6-ring PAHs were dominant, especially those of 4-ring PAHs, which were above 30% of the total PAHs in each season. Source apportionment indicated that PM<sub>2.5</sub>-bound PAHs in Huangshi were mainly derived from pyrogenic source, vehicle exhaust, coal combustion, and biomass burning. Incremental lifetime cancer risks (ILCRs) showed no potential carcinogenic risk from the PM<sub>2.5</sub>-bound BaP-eq. ILCRs in winter were the highest, and the risks for adults were approximately an order of magnitude higher than those for children.

**Keywords** PAHs · Particulate matter (PM) · Industrial city · Seasonal variations · Health risk assessment

## Introduction

Problems in atmospheric pollution, such as photochemical smog in Los Angeles and a smoke incident in London, have

**Electronic supplementary material** The online version of this article (<https://doi.org/10.1007/s11869-018-0575-3>) contains supplementary material, which is available to authorized users.

✉ Jiaquan Zhang  
jiaquanzh@163.com

- <sup>1</sup> School of Environmental Science and Engineering, Hubei Key Laboratory of Mine Environmental Pollution Control and Remediation, Hubei Polytechnic University, Huangshi 435003, China
- <sup>2</sup> State Key Laboratory of Biogeology and Environmental Geology, School of Environmental Studies, China University of Geosciences, Wuhan 430074, China
- <sup>3</sup> Key Laboratory of Aerosol Chemistry and Physics, Institute of Earth Environment, Chinese Academy of Sciences, Xi'an 710075, China

aroused widespread concern (Lee et al. 2008). With rapid expansion of the world's population and the global economy, urbanization and industrialization have increasingly developed, problems in atmospheric pollution have exacerbated, and atmospheric particulate matter has strongly affected air quality, human health, and climate (Xu et al. 2016). The negative effects of PM, especially PM<sub>2.5</sub>, on cardiovascular and respiratory diseases are well documented (Leitte et al. 2011). Epidemiological studies have reported that exposure to PM<sub>2.5</sub> decreases lung function and exacerbates respiratory symptoms, such as irritation of the airways, coughing, or difficulty in breathing (Correia et al. 2013). Globally, China has one of the highest PM<sub>2.5</sub> levels (Kim et al. 2015) and has recorded frequent haze occurrence. Thus, atmospheric pollution is urgent to be solved.

Among all chemical components of PM, carbon particles, including organic, elemental, and inorganic carbons, affect air quality, visibility, and climate change; the content of inorganic carbon is lower than those of other carbon particles and thus generally ignored (Decesari et al. 2000). Organic carbon is

found in many organic compounds, including PAHs, *n*-alkanes, organic acids, carbonyl compounds (aldehydes and ketones), and heterocyclic compounds (Yang et al. 2003). Most of these compounds are toxic to health, and some are even highly carcinogenic (Blaszczuk et al. 2017); furthermore, the hydrophilicity of water-soluble organic carbon influences the moisture removal of atmospheric particulates and the formation of fog (Novakov and Penner 1993). Among organic carbons, PAHs show the most consistent association with adverse health outcomes (Xing et al. 2016; Xu et al. 2016) because of their high durability and toxic effects, such as carcinogenic, teratogenic, and mutagenic characteristics (Blaszczuk et al. 2017; Xing et al. 2011). PAHs can through the global distillation effect and “the grasshopper jumped effect” for long-range migration in the atmospheric environment and cause global pollution because of their semi-volatile characteristics (Wania and Mackay 1995; Wania and Mackay 1996). Carbonaceous particles, especially PAHs, not only affect visibility and air quality and climate change but also pose serious threat to human health because their main enrichment in fine particle size likely allows them to penetrate the human respiratory system. Moreover, most organic components are toxic and may be associated with many diseases, such as cancer and respiratory diseases, decreased lung function, and reduced immunity (Bari et al. 2010; Leitte et al. 2011).

In China, rapid economic and industrial development has resulted in severe problems in atmospheric pollution in its major cities with negative consequences on the health of its population, high healthcare costs, and associated loss of economic productivity. The effect of atmospheric pollution includes approximately 300,000 premature deaths per year, and the costs of treatment for illnesses caused by air pollution corresponded to 4% of China’s gross domestic product in 2003. According to the global burden disease assessment, atmosphere pollution in China in 2010 caused more than 1.2 million premature deaths and a loss of more than 25 million healthy lives, and these values were equivalent to a 33% increase from the estimates in 1990 (Yang et al. 2013). A series of studies on PM-bound PAHs in China, such as Zhang and Tao (2008), has revealed that the concentration of PAHs in winter is more than that in summer because of solid fuel consumption. Lai et al. (2011) found that summer monsoon activities contribute to the diffusion of atmospheric pollutants, thereby reducing the concentration of PAHs. PM-bound PAHs in Nanjing (Chen et al. 2013), Beijing (Niu et al. 2016), and Guangzhou (Liu et al. 2015) have also been investigated. However, many research has mainly focused on large and northern industrial cities, such as the Pearl River Delta in southern city, less attention was paid to the mining transformation of the central city.

The objectives of our work were (1) to determine the temporal course and seasonal variation in PM<sub>2.5</sub>-bound concentrations and composition pattern of PAHs from a typical mining

city urban site in central China for seasonal variations, (2) to assess the sources and influence of meteorological conditions on the PM<sub>2.5</sub> concentrations of PAHs, and (3) to estimate the potential health impact of PM<sub>2.5</sub> on the inhabitants of this urban center and the temporal and seasonal variations in PM<sub>2.5</sub>.

## Methodology

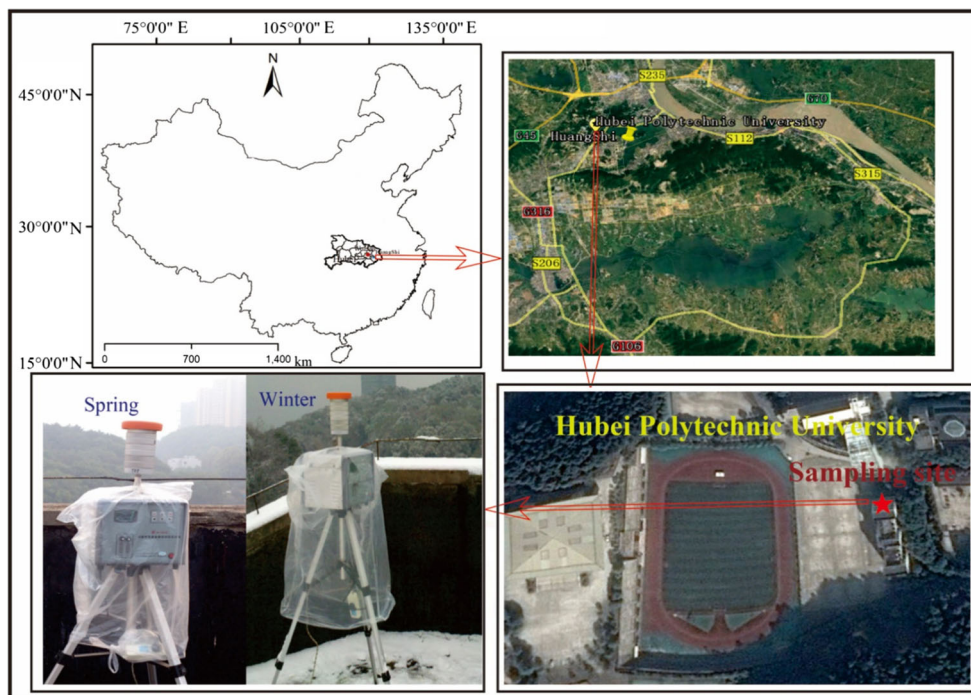
### Sampling

The PM<sub>2.5</sub> sampler was located at the roof top of the fifth floor building hosting the School of Environmental Science and Engineering of Hubei Polytechnic University (approximately 16 m above the ground) in 2013 and central Huangshi (Fig. 1). PM<sub>2.5</sub> (24-h samples) were collected for about 15 days (Table S1) in each season (from 9:00 a.m. to 9:00 a.m. on the next day) on pre-baked (450 °C for 3 h) glass fiber filters (GF/F, ø 90 mm, Whatman, UK) using a TH-150c median volume PM<sub>2.5</sub> air sampler (Wuhan Tianhong instruments Co., Ltd., Wuhan, China) at a flow rate of 100 L/min. A total of 60 samples were collected. PM<sub>2.5</sub> masses were determined by weighing before and after sampling with a one in a million electronic balance under constant temperature (25 °C) and relative humidity (50%). Field blanks were collected to eliminate the passive adsorption of gas-phase organic compounds onto the filter during and/or after sampling. All sampled filters were stored at –15 °C after sampling until their analysis. Meteorological data, such as ambient temperature, pressure, and relative humidity, were recorded during sampling.

### Analysis of PAHs

A total of 16 USEPA priority PAHs: naphthalene (Nap), acenaphthylene (Acy), acenaphthene (Ace), fluorene (Flu), phenanthrene (Phe), anthracene (Ant), fluoranthene (Fla), pyrene (Pyr), benzo[a]anthracene (BaA), chrysene (Chr), benzo[b]fluoranthene (BbF), benzo[k]fluoranthene (BkF), benzo[a]pyrene (BaP), indeno[1,2,3-cd]pyrene (IcdP), dibenzo[a,h]anthracene (DBA), and benzo[g,h,i]perylene (BghiP), were measured.

Half of the filter sample was spiked with 5 µL (200 µg/mL) mixed-recovery surrogates (naphthalene-d<sub>8</sub>, acenaphthene-d<sub>10</sub>, phenanthrene-d<sub>10</sub>, chrysene-d<sub>12</sub>, and perylene-d<sub>12</sub>), and the spiked sample was then extracted with dichloromethane (DCM) using soxhlet apparatus for 24 h. Elemental sulfur was removed by adding activated copper granules to the collection flasks. The sample extract was concentrated and the solvent exchanged to hexane and further reduced to 2–3 mL by using a rotary evaporator (Heidolph4000, Germany). A 1:2 (v/v) alumina/silica gel column (48 h extraction with DCM, then 180 and 270 °C muffle drying for 12 h, both deactivated 3% with H<sub>2</sub>O before use) was used to clean-up the extract.

Fig. 1 PM<sub>2.5</sub> sampling site

Then, the PAHs were eluted with 30 mL of DCM/hexane (2:3). The eluate was concentrated to 0.2 mL under a gentle nitrogen stream. Prior to analysis, a known quantity (1000 ng) of hexamethylbenzene was added to the eluates as an internal standard.

PAHs were analyzed by using a gas chromatograph-mass spectrometer (GC-MS, 7890A/5975MSD, Agilent Technologies, Santa Clara, CA, USA) equipped with a DB-5 capillary column (30 m × 0.25 mm i.d × 0.25 μm film thickness). The instrument was operated using electron impact (EI) ionization at 70 eV and in the selected ion monitoring (SIM) mode. The chromatographic conditions were as follows: The injector and detector temperatures were 270 and 280 °C, respectively. The oven temperature program was kept at 60 °C for 5 min and increased to 290 °C at a rate of 5 °C/min and kept at 290 °C for 20 min. The high-purity He carrier gas was delivered at a constant flow rate of 1.0 mL/min.

### Quality assurance and quality control

Procedural blanks, spiked blanks, and sample duplicates (analyzed at a rate of 10% of the total samples) were analyzed to evaluate the precision of the analyses. The PAHs found in the field blanks were generally below the limits of detection (LOD), which was defined as the amount of an analyte that would generate a signal-to-noise ratio of 3:1. No target PAHs were detected in any of the procedural blanks. The variations in PAH concentrations in duplicate samples were less than 15%. Minimum detection limits (MDLs) for the 16 PAHs were in the range of 0.01–0.47 ng (Table S2). Representative

average percentage recoveries (arithmetic mean ± standard deviation, SD) were 58 ± 6%, 82 ± 9%, 108 ± 10%, 112 ± 13% and 118 ± 11% for naphthalene-d<sub>8</sub>, acenaphthene-d<sub>10</sub>, phenanthrene-d<sub>10</sub>, chrysene-d<sub>12</sub>, and perylene-d<sub>12</sub>, respectively. The final data were corrected by the recovery rate.

### Analysis of WTOC and WTN

One eighth of each sample was extracted with 15 mL deionized water. Then, the extracts were filtered by a glass fiber microporous membrane filter with a diameter of 0.45 μm. The strained liquid were frozen and stored at −15 °C prior to the analysis of the water-solubility total organic carbon (WTOC) and water-solubility total nitrogen (WTN), respectively. WTOC and WTN were measured using a Multi N/C 2100-H1100 analyzer (Analytic Jena, Germany).

### Carcinogenic risk assessment

The risk of cancer because of being exposed to particular PAH was expressed in terms of BaP, as the toxic equivalence factor (TEF), because humans are exposed to complex PAH mixtures (Chen et al. 2017). The 16 PAH TEFs were used in the calculation. The sum of the products of each PAH concentration and its respective TEF are called BaP<sub>-eq</sub> value. BaP<sub>-eq</sub> was calculated for PM<sub>2.5</sub> samples of Huangshi City using Eq. (1).

$$\text{BaP}_{\text{-eq}} = \sum \text{PAH}_{\text{conc}} \times \text{PAH}_{\text{TEF}} \quad (1)$$

Where BaP<sub>-eq</sub> is the BaP-based toxic equivalency factor, PAH<sub>conc</sub> is the concentration of individual PAH, and

PAH<sub>TEF</sub> is the toxic equivalent factor of individual PAH using the factors proposed by Nisbet and LaGoy factors (Nisbet and Lagoy 1992).

Health risk can be estimated using PAH exposure through inhalation (Chen et al. 2017). The incremental lifetime cancer risks (ILCRs) in human beings can be quantitatively calculated on the basis of the lifetime average daily dose (LADD) of PAHs. The Eqs. (2) and (3) are used to calculate LADD and ILCRs:

$$\text{LADD} = C \times \text{IR} \times \text{ED} \times \text{EF} / (\text{BW} \times \text{ALT}) \quad (2)$$

$$\text{ILCRs} = \text{LADD} \times \text{CSF} \quad (3)$$

where the parameters used to estimate the ILCRs listed in Table 1 (Chen et al. 2017; Li et al. 2016).

### Statistical analysis

Correlation analyses, principal component analyses (PCA), and other statistical procedures were applied by using SPSS 22.0 and Origin 9.0. PCA analyses were used to identify presumptive sources for the PAHs.

## Results and discussion

### PM<sub>2.5</sub> and PAH concentrations

Statistics of the annual mean concentrations of PM<sub>2.5</sub>, individual and total PAHs in PM<sub>2.5</sub> as well as the meteorological conditions during the whole sampling period are shown in Table 2.

The concentrations of PM<sub>2.5</sub> for the entire sampling period were in the range of 6.96 to 260.06  $\mu\text{g}/\text{m}^3$  with a mean of 177.05  $\mu\text{g}/\text{m}^3$ . Only 38% of the sampling days exceeded the 24-h limit value that was set in the ambient air quality standards (AAQs), which is 75  $\mu\text{g}/\text{m}^3$  in China (GB3095-2012). During autumn and winter, nearly all the sampling days overtopped the 75  $\mu\text{g}/\text{m}^3$  24-h limit value, and the concentration of PM<sub>2.5</sub> aerosols only exceeded the 24-h WHO PM<sub>2.5</sub>

**Table 2** Summary of the average PM<sub>2.5</sub> ( $\mu\text{g}/\text{m}^3$ ), total PAH ( $\text{ng}/\text{m}^3$ ), WTCO ( $\mu\text{g}/\text{m}^3$ ), WTN ( $\mu\text{g}/\text{m}^3$ ) concentrations, and meteorological conditions (Tem = temperature: °C, R H = relative humidity: %, WTCO = water-solubility TOC, WTN = water-solubility TN)

	Ring	TEF	Min	Max	Mean	SD
Tem			1.50	35.00	19.57	10.57
R H			40.00	98.00	80.00	13.00
PM <sub>2.5</sub>			6.96	260.04	117.05	66.46
Nap	2	0.001	N.D.	2.41	0.50	0.53
Acy	3	0.001	N.D.	0.13	0.05	0.03
Ace	3	0.001	N.D.	0.02	0.00	0.01
Flu	3	0.001	N.D.	0.13	0.01	0.03
Phe	3	0.001	N.D.	2.27	0.76	0.64
Ant	3	0.01	N.D.	0.23	0.01	0.04
Fla	4	0.001	0.22	7.95	1.76	1.59
Pyr	4	0.001	0.06	6.19	1.20	1.22
BaA	4	0.1	N.D.	6.32	0.82	1.06
Chr	4	0.01	N.D.	5.23	0.82	1.00
BbF	5	0.1	N.D.	3.14	0.66	0.83
BkF	5	0.1	N.D.	1.72	0.46	0.46
BaP	5	1	N.D.	1.89	0.48	0.50
DBA	5	1	0.35	1.20	0.52	0.17
IcdP	6	0.1	0.04	5.04	1.50	1.38
BghiP	6	0.01	N.D.	6.53	1.09	1.08
$\Sigma\text{PAHs}$			1.51	44.51	10.65	8.86
WTCO			40.68	1229.10	124.81	156.45
WTN			9.30	431.53	54.69	56.38

SD standard deviation; N.D. not detected or below the detection limit;  $\Sigma\text{PAHs}$  16 individual PAHs

guideline of 25  $\mu\text{g}/\text{m}^3$  once in all other days (WHO 2005) during the whole sampling period. The highest average concentration was 3 times of the AAQs limit value and more than 40 times of the lowest value with great scattering, suggesting that the PM<sub>2.5</sub> pollution in Huangshi may be seriously influenced by local pollution sources. PM<sub>2.5</sub> mass concentrations in Huangshi were comparable to those measured in 2013 in Wuhan (114.9  $\mu\text{g}/\text{m}^3$ , mean, same as below) (Zhang et al. 2015a), but lower than those measured in Zhengzhou

**Table 1** Parameters used to estimate the ILCRs

Parameter	Meaning	Value	
		Adult	Children
C ( $\text{mg}/\text{m}^3$ )	PAHs concentration in PM <sub>2.5</sub>	LADD instead of C	
IR ( $\text{m}^3/\text{day}$ )	Air inhalation rate	20	7.6
ED (years)	Lifetime exposure duration	52	6
EF (days/year)	Exposure frequency	2	
BW (kg)	Body weight	70	15
ALT (days)	Average lifetime	70 years $\times$ 365 day year = 25,550 days	
CSF ( $\text{mg}/(\text{kg} \times \text{day})$ )	Cancer slope factor	3.14	

(114.9  $\mu\text{g}/\text{m}^3$ ) (Geng et al. 2013) and Chengdu (114.9  $\mu\text{g}/\text{m}^3$ ) (Tao et al. 2013) and higher than those in Xi'an, Beijing, Guangzhou, Ostrava, Czech Republic, Houston, USA, Zaragoza, and Spain (Table S3). These findings proved once more that the  $\text{PM}_{2.5}$  pollution in Huangshi was serious and control measures should be taken to alleviate it.

With regard to PAH, the concentrations of  $\text{PM}_{2.5}$ -bound PAHs in the whole sampling period were between 1.51 and 44.51  $\text{ng}/\text{m}^3$  with a mean of 10.65  $\text{ng}/\text{m}^3$ . The total PAHs accounted for 0.002 to 0.104% of the  $\text{PM}_{2.5}$  mass, which were lower than those in Xi'an (0.04% to 0.11%) (Xu et al. 2016).  $\text{PM}$ -bound PAHs in China have no regulatory standard or guideline, thus, our study was compared with the works of other researchers for assessment (Table S3). The average concentrations of PAHs in  $\text{PM}_{2.5}$  were lower by 33.89  $\text{ng}/\text{m}^3$  in Guangzhou, 57.1  $\text{ng}/\text{m}^3$  in Xi'an, 61.2  $\text{ng}/\text{m}^3$  in Beijing, and 99.9  $\text{ng}/\text{m}^3$  in Ostrava, Czech Republic but more than twice or 4.59  $\text{ng}/\text{m}^3$  in Hongkong, much higher by 2.79  $\text{ng}/\text{m}^3$  in Bangi, Malaysia, 2.14  $\text{ng}/\text{m}^3$  in Zaragoza, Spain, 3.80  $\text{ng}/\text{m}^3$  in Rio de Janeiro, Brazil, 3.16  $\text{ng}/\text{m}^3$  in Atlanta, USA, and one order of magnitude higher than those in Houston, USA, which was 0.31  $\text{ng}/\text{m}^3$ .

### Seasonal variation

The seasonal distribution of particle-bound PAHs depends on a variety of comprehensive factors, such as radiation and dispersion conditions (Beyer et al. 2003). The mass concentrations of  $\text{PM}_{2.5}$ , and the concentrations of PAHs in  $\text{PM}_{2.5}$  all showed distinct seasonal variations in Huangshi (Fig. 2), and a Pearson's correlation analysis was conducted to understand the correlation among the  $\text{PM}_{2.5}$ , PAHs, and meteorological variables, as shown in Table S4.

The mass concentrations of  $\text{PM}_{2.5}$  manifested a tendency that winter (mean 189.25  $\mu\text{g}/\text{m}^3$ ) > autumn (mean 150.81  $\mu\text{g}/\text{m}^3$ ) > spring (mean 67.13  $\mu\text{g}/\text{m}^3$ ) > summer (mean 52.87  $\mu\text{g}/\text{m}^3$ ) (Fig. 2). Seasonal trends were likely attributed to meteorological conditions and human activities. In spring, summer, autumn, and winter, 40, 6.25, 93.75, and 100% of daily  $\text{PM}_{2.5}$  mass concentrations were higher than 75  $\mu\text{g}/\text{m}^3$  (the level II standard of AAQs in China), respectively. In summer, Huangshi was influenced by the West Pacific subtropical high, frequent heavy or torrential rain, which was an efficient way to remove particles from the atmosphere. Furthermore, precipitation conditions, which have advantages to atmospheric diffusion, can decrease the enrichment of air pollutants (Zhang et al. 2015b). The Spearman correlation analysis showed a weak negative correlation between  $\text{PM}_{2.5}$  and relative humidity (R.H) but observed a significant negative correlation ( $r = -0.78$ ,  $p < 0.01$ , Table S4) between the  $\text{PM}_{2.5}$  and the temperature, confirming that the mass concentrations of  $\text{PM}_{2.5}$  were not affected by single meteorological factors again.

PAHs have the same tendency as the  $\text{PM}_{2.5}$ , that is, winter (mean 22.56  $\text{ng}/\text{m}^3$ ) > autumn (mean 9.57  $\text{ng}/\text{m}^3$ ) > spring (mean 5.31  $\text{ng}/\text{m}^3$ ) > summer (mean 4.03  $\text{ng}/\text{m}^3$ ). The weather in Huangshi City is dry and hot during summer and wet and cold during winter. The average concentrations of PAHs in winter are approximately 5.6 times higher than those during summer. However, meteorological variables, such as temperature, have an exactly opposite change tendency, that is, summer > spring > autumn > winter distribution. The Spearman correlation analysis showed the same significant negative correlation ( $r = -0.79$ ,  $p < 0.01$ , Table S4) between PAHs and temperature as the  $\text{PM}_{2.5}$  and temperature. During summer, high temperature, and strong radiation may lead transform PAHs from particulate phase into vapor phase, whereas the decrease in ambient temperature enhances the condensation of gas-phase PAHs onto atmospheric particles (Callen et al. 2014), thereby resulting in a negative correlation between PAHs and temperature. Furthermore, high temperatures and strong solar radiation can cause strong photochemical decomposition and might promote the degradation of PAHs (Beyer et al. 2003; Panther et al. 1999), and erosion of rainfall simulator, and the summer monsoon (Karar and Gupta 2006) can also result in lower PAHs concentrations in summer than in other seasons. Frequent human activities, such as domestic heating, have contributed to the increase of particulate-bound PAH concentrations during the cold season (Callen et al. 2014).

### WTOC and WTN and $\text{PM}_{2.5}$ and PAHs

Surface tension decreases because of the soluble organic carbon in moisture sol and cloud droplets and may affect the gas-liquid interface and nucleation of cloud droplets; moreover, the growth and compounding of cloud droplets have important influence on cloud formation (Decesari et al. 2000; Shulman et al. 1996). However,  $\text{PM}$ -bound PAHs can only be removed by atmospheric dry and wet deposition and rainfall.

The concentrations of WTOC and WTN in  $\text{PM}_{2.5}$  are shown in Fig. S1. During the whole sampling period, the mass concentrations of WTOC was between not detected (ND) to 19.86  $\mu\text{g}/\text{m}^3$  with a mean of 7.84  $\mu\text{g}/\text{m}^3$ , which was the highest value that existed in autumn, whereas, the lowest value existed in spring and summer. WTN between 0.14 to 16.15  $\mu\text{g}/\text{m}^3$ , with a mean of 5.73  $\mu\text{g}/\text{m}^3$ . WTOC and WTN in autumn and winter were significantly higher than during spring and summer. The concentrations of WTOC accounted for 0.00 to 79.21% of the  $\text{PM}_{2.5}$  mass, and WTN accounted for 0.27 to 38.08% of the  $\text{PM}_{2.5}$  mass (Fig. S2). Correlation coefficients matrix among the individual PAHs, WTOC, and WTN in Table S4 showed that 3-, 4-, 5-, 6-ring PAHs were significantly correlated with one another, and WTOCs were significantly negatively correlated with the HMW-PAHs (e.g.,

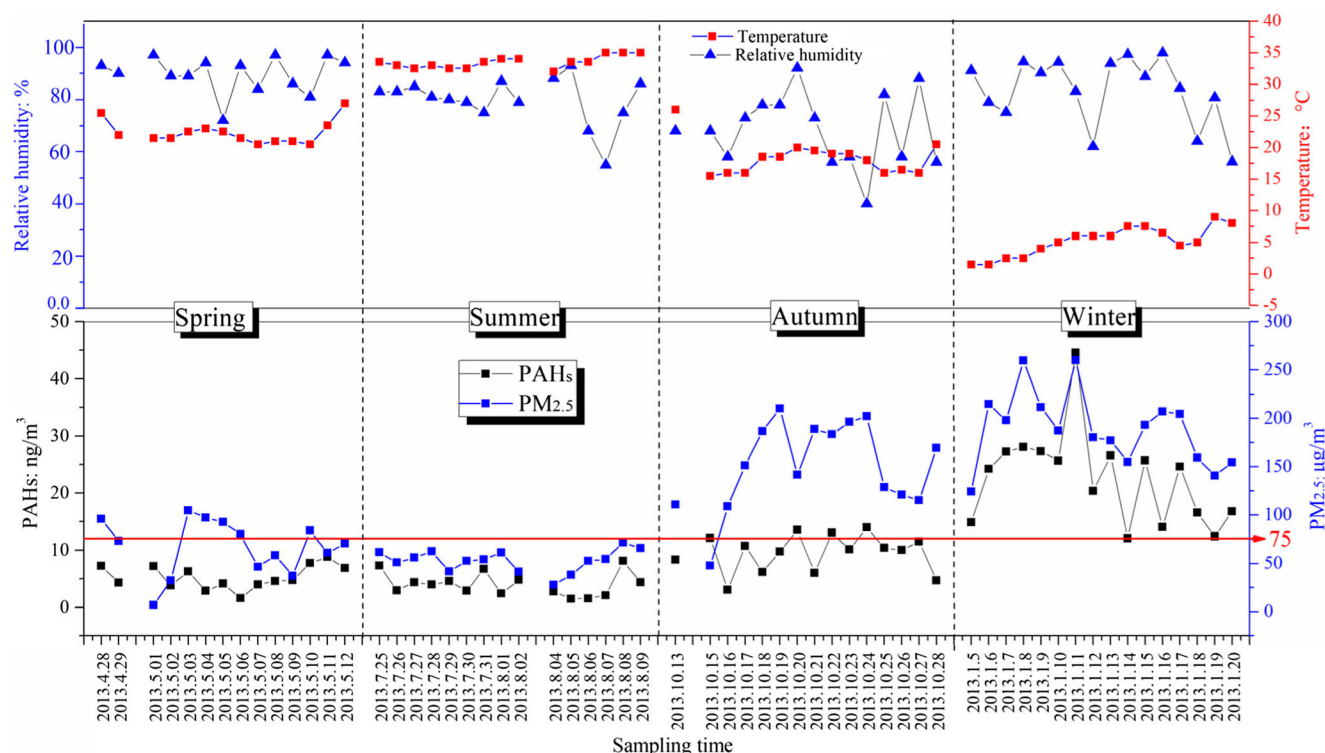


**Fig. 2** Seasonal variation of  $PM_{2.5}$  and PAHs in  $PM_{2.5}$  and meteorological variables

4-, 5- and 6-ring PAHs). The WTNs were significantly correlated with HMW-PAHs (including 4-, 5-, and 6-ring PAHs). The effects of WTN and WTOC were exactly opposite. TOC is essential for the sorption, sequestration, and fate of PAHs (Günther et al. 1996).

### Composition of PAHs in $PM_{2.5}$

The compositions of PAHs in  $PM_{2.5}$  are shown in Fig. 3. The average concentrations of PAHs have the decreasing order of Fla. > IcdP > Pyr > BghiP > Chr = BaA > Phe > BbF > DBA > Nap > BaP > BkF > Acy > Flu = Ant > Ace over all sampling periods. The 2-, 3-, 4-, 5-, and 6-ring PAHs account for 7.66, 9.92, 38.14, 20.71, and 23.56% of the total PAHs, respectively. The 4-, 5-, and 6-ring PAHs (HMW-PAHs) were dominant in each sampling season. Furthermore, the concentrations of HMW-PAHs were the highest in winter, followed by autumn, which accounted for 91.40 and 87.45% of the total PAHs, respectively. The average concentrations of 4-ring (each season was above 30%) PAHs in every season are higher than 5- and 6-ring PAHs. The concentrations of LMW-PAHs account for 19.23 and 28.95% of the total PAHs in spring and summer, respectively. The percentage LMW-PAHs in summer was approximately 34 times higher than that in winter. The production of different molecular weights of PAH in gas or particle was different. Previous studies suggest that high temperature and strong radiation may transform PAHs from particulate phase into vapor phase,

whereas low temperature enhances the condensation of gas-phase PAHs onto atmospheric particles (Callen et al. 2014). More than 90% of LMW-PAHs were found in the gas phase because of their high vapor pressure and strong volatility. More than 90% of HMW-PAHs were present in the particle phase because of its low vapor pressure; as a result, the LMW-PAHs might have a higher proportion in the gas phase than those of the HMW-PAHs (Augusto et al. 2010; Bandowe et al. 2014). Therefore, the highest concentrations of LMW-PAHs and HMW-PAHs were found in summer and winter, respectively, for the yearly changes of the highest and lowest temperatures in Huangshi.

### Source apportionment of PAHs in $PM_{2.5}$

Compositional pattern, molecular composition, and principal component analyses were used to identify the possible sources of PAHs in  $PM_{2.5}$ . The identification of possible sources of PAHs is important not only for understanding the patterns in the data from this study but also for developing scenarios of what to expect when emissions change in the future.

### Composition pattern analysis

Two of the main anthropogenic sources of PAHs are combustion processes and the incomplete combustion of petroleum products (Xing et al. 2011). For PAHs released by combustion, LMW-PAHs are produced primarily at low to moderate

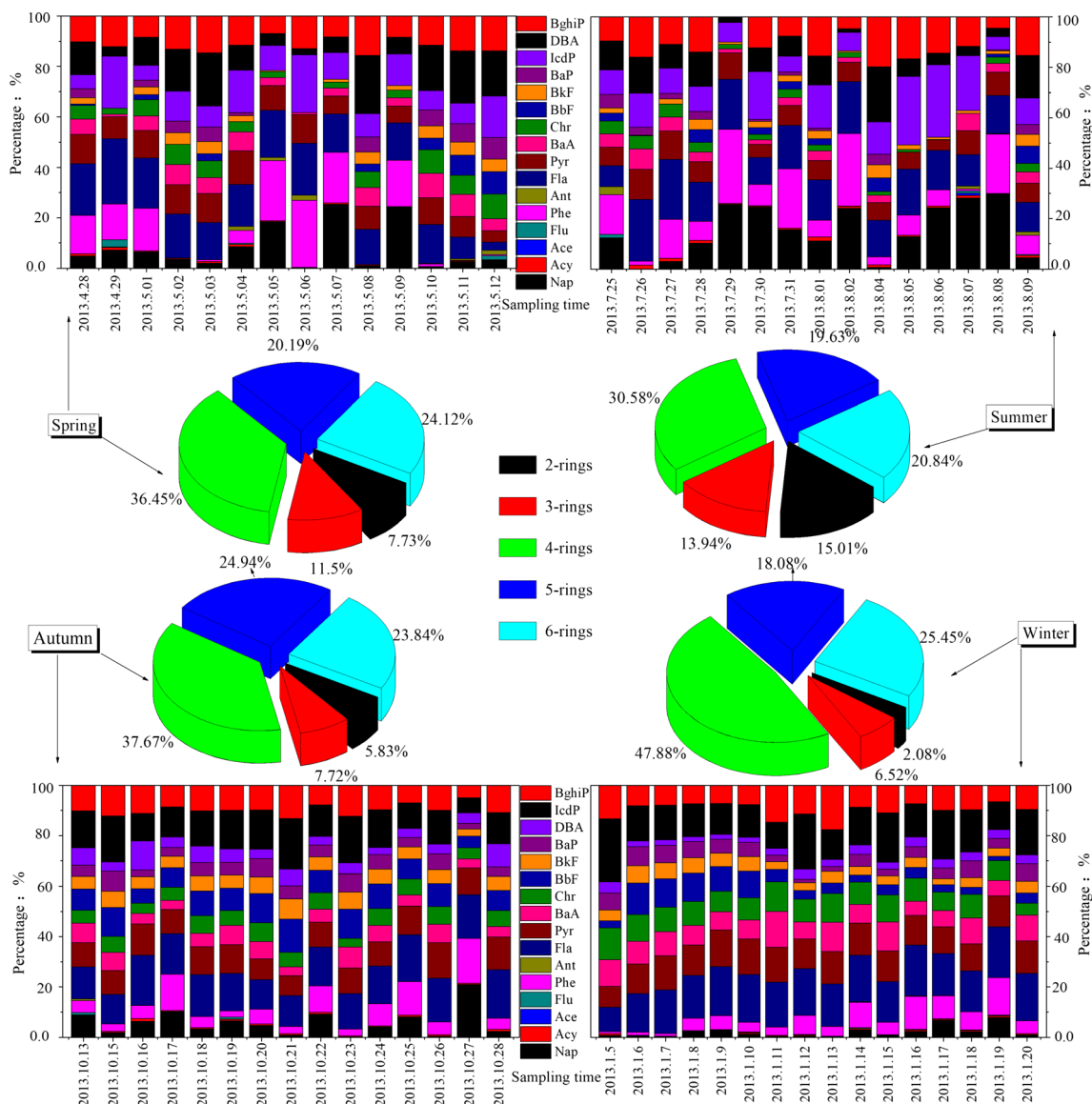


Fig. 3 Composition of PAHs in PM<sub>2.5</sub> for the four seasons

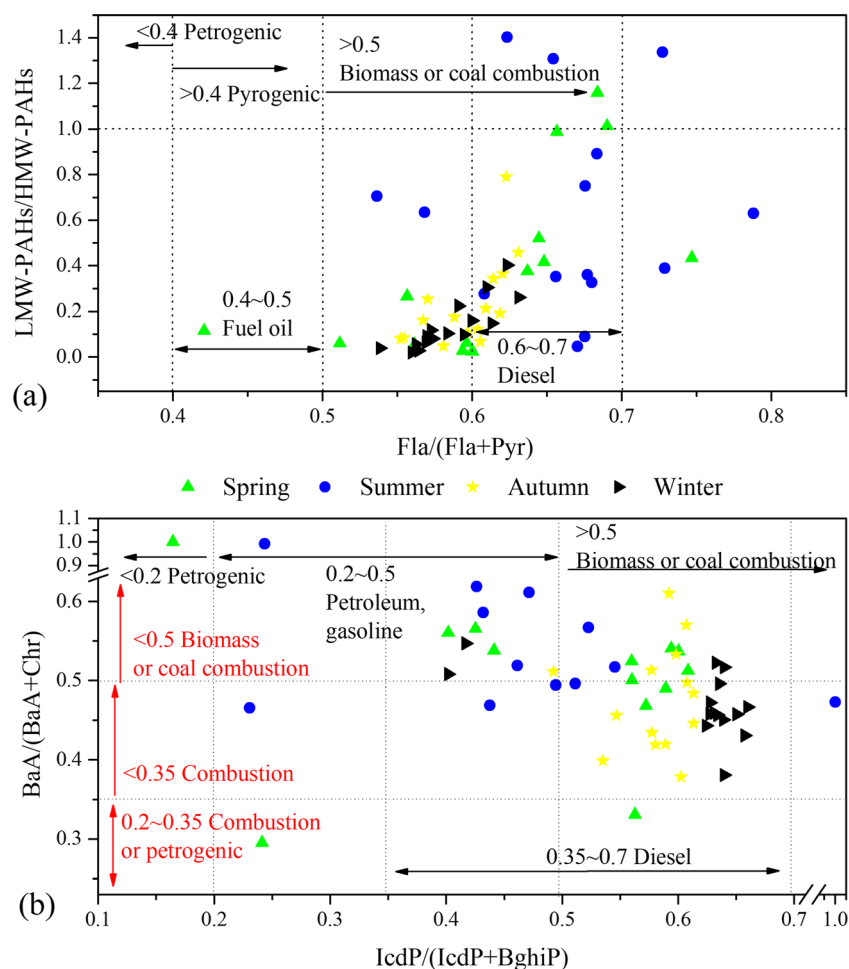
temperatures, whereas HMW-PAHs are generated at high temperatures (Xing et al. 2011). Therefore, large relative abundances of LMW-PAHs indicate that most of the PAHs originated from petrogenic sources, whereas high, relative abundances of HMW-PAHs can be explained by greater impacts from pyrogenic sources. In our study, the average LMW/HMW-PAHs ratios during the entire sampling periods were below 1, except 3 days in summer and 2 days in spring (Fig. 4a), indicating that the PAHs in Huangshi were greatly derived from pyrogenic sources.

**Diagnostic ratios analysis**

Diagnostic ratios based on ratios of individual PAH congeners have been used to discriminate between petrogenic and pyrolytic sources. In particular, the ratios of BaP BghiP,

Ant (Ant + Phe), Flu (Flu+Pyr), Fla. (Fla + Pyr), IcdP (IcdP + BghiP), and BaA (BaA + Chr) have been used for this purpose (Li et al. 2016; Xu et al. 2016; Yunker et al. 2002; Zhang et al. 2016). Scatterplot of the ratios of selected PAH congeners were drawn based on the principle of molecular indices (Xing et al. 2011), and these PAH congener-pair relationships were used to evaluate the PAH sources further. In this study, the ratios of IcdP (IcdP + BghiP) V&S BaA (BaA + Chr) and Fla. (Fla + Pyr) were used to identify sources of PAHs in PM<sub>2.5</sub> because some individual PAHs were below the LOD or ND. The ratio of BaA (BaA + Chr) > 0.35 implies combustion source, values >0.5 implies biomass or coal combustion source, and values <0.2 implies petroleum source, and values between 0.2 and 0.35 imply petroleum combustion source (Khan et al. 2015; Zhang et al. 2015b). Furthermore, IcdP (IcdP + BghiP) ratios >0.5 indicate

**Fig. 4** Scatterplot of molecular indices used to identify PAH sources: **a** Fla. (Fla + Pyr) versus LHM-PAHs/HMW-PAHs and **b** BaA (BaA + Chr) versus IcdP (IcdP + BghiP)



biomass or coal combustion source, ratios  $< 0.2$  indicate petroleum source and ratios between 0.2 and 0.5 indicate petroleum combustion source and ratios between 0.35 and 0.7 indicate diesel source. Moreover, the ratio of Fla. (Fla + Pyr)  $> 0.5$  manifest biomass or coal combustion source, in the range of 0.4–0.5 manifest fuel oil, and values  $< 0.4$  manifest petrogenic source (Hu et al. 2017; Li et al. 2016; Yunker et al. 2002).

In this study, the ratios of selected PAH congeners scatterplots (Fig. 4) showed that the ratio of Fla. (Fla + Pyr) (Fig. 4a) was higher than 0.5, except 1 day in spring, which was 0.42, indicating that the PAHs in  $PM_{2.5}$  were derived from pyrogenic source, and biomass or coal and diesel were the main source of combustion. The diagnostic values of IcdP (IcdP + BghiP) (Fig. 4b) were higher than 0.2, and most values were higher than 0.35 during the sampling periods. These findings confirmed that these representative HMW-PAHs came from fuel combustion sources, especially during autumn and winter, in which the ratios of IcdP (IcdP + BghiP) were all mostly above 0.5, implying that its source was from biomass or coal. Nearly all of the ratios of BaA (BaA + Chr) were between 0.36 and 1.0, above 0.5, except 2 days in spring. Therefore, the major source was combustion.

The molecular diagnostic ratios of PAHs indicated that the PAHs in  $PM_{2.5}$  were mainly derived from pyrogenic sources. The activity of the local population was undoubtedly the greatest source of PAH pollution in the area. For instance, the Golden Mountain economy and Jinshan coal development zone were located in the south of the Huangshi, in the southeast and southwest of the city, a garbage incineration power plant and Cisse mountain coal-fired power plant were found, respectively. In addition, Huangshi is not only a mining city but is also the cradle of steel and the base of aluminum in our country. These industrial and mining enterprises consume large amounts of energy and release large amounts of pollutants. However, sources of PAHs are evidently complicated and the concentrations of PAHs are affected by many factors, including industry, transportation, and human daily life.

### Principal component analysis

Figure 6 shows the PCA factor loadings, in which three factors were extracted during spring, summer, autumn, and winter, accounting for 84.95, 84.68, 88.62, and 83.78% of the total variance, respectively.

Spring: factor 1 was highly loaded with BaA, Chr, BbF, BkF, BaP, IcdP, and BghiP, accounting 48.32% of the total variance. Chen et al. (2017) and Rogge et al. (1993) suggested that HMW-PAHs were mainly related to vehicle emission (Larsen and Baker 2003), and also suggested that PAH species rest with the combustion temperature; HMW-PAHs prevail in high-temperature (e.g., vehicle emissions) and complete combustion; nevertheless, at low to moderate temperatures (e.g., coal and biomass combustion), LMW-PAHs are abundant (Zhang et al. 2015b). Therefore, factor 1 significantly indicated traffic emission source. Factor 2 indicated coal and biomass combustion source with high loading of Ant Fla. and Pyr (Khalili et al. 1995) and accounted for 20.02% of the total variance. Previous studies suggested that Ant was a marker of coal combustion source (Fraser et al. 1997), and Fla. and Pyr originated from biomass burning (Khalili et al. 1995). Factor 3 indicated coal combustion and vehicle emission source, accounting for 16.61% of the total variance and highly loaded with Ace, Flu, and DBA. Although Ace and Flu were the markers of coal combustion source (Chen et al. 2017; Khalili et al. 1995),

DBA has been widely used as a tracer for gasoline and diesel exhaust (Hu et al. 2017; Yunker et al. 2002).

Summer: factor 1 accounted for 30.49% of the total variance and was highly loaded with Acy, BkF, IcdP, and BghiP. It was interpreted as traffic emission source. Factor 2 accounted for 27.29% of the total variance and with high loading of Flu, Ant, BaP, and DBA. Factor 2 was interpreted as coal combustion and traffic emission source. As mentioned previously (Chen et al. 2017; Fraser et al. 1997; Khalili et al. 1995), BaP and DBA have been widely used as a tracer for gasoline and diesel exhaust (Hu et al. 2017; Yunker et al. 2002). Factor 3 was interpreted as biomass combustion source, accounting for 26.90% of the total variance and was highly loaded with Nap, Phe, Fla., and Pyr, as Khalili et al. (Khalili et al. 1995), Yunker et al. (Yunker et al. 2002), and Chen et al. (Chen and Liao 2006) mentioned that Nap, Phe, Fla., and Pyr originated from biomass burning.

Autumn: factor 1 was interpreted as traffic emission source, accounting for 46.16% of the total variance and was highly loaded with BaA, Chr, BbF, BkF, BaP, IcdP, and BghiP. Factor 2 was interpreted as biomass combustion source, accounting

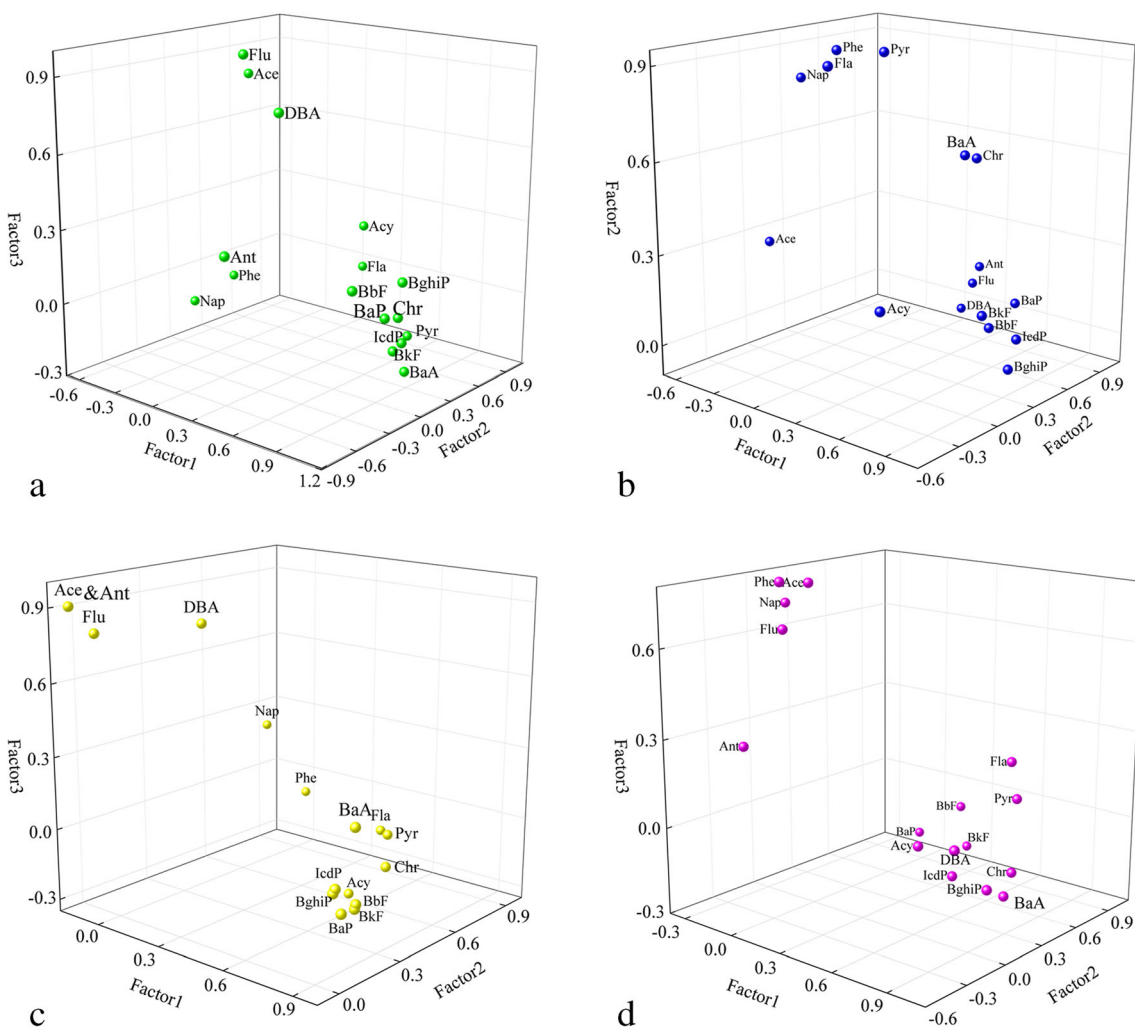


**Fig. 5** Factor loadings of 3D PCA plots. **a** Spring. **b** Summer. **c** Autumn. **d** Winter

for 21.80% of the total variance and was highly loaded with Nap, Phe, and Fla. Factor 3 was interpreted as coal combustion source, accounting for 20.65% of the total variance and was highly loaded with Ace, Flu, and Ant.

Winter: factor 1 accounted for 35.75% of the total variance and was highly loaded with Acy, Fla., Pyr, BaA, Chr, DBA, IcdP, and Bghip. Thus, factor 1 was interpreted as biomass combustion and traffic emission source. Factor 2 accounted for 25.20% of the total variance and was highly loaded with BbF, BkF, and BaP. Therefore, factor 2 was interpreted as traffic emission. Factor 3 accounted for 22.83% of the total variance and was highly loaded with Nap, Ace, and Phe. Thus, factor 3 was interpreted as coal and biomass combustion source (Fig. 5).

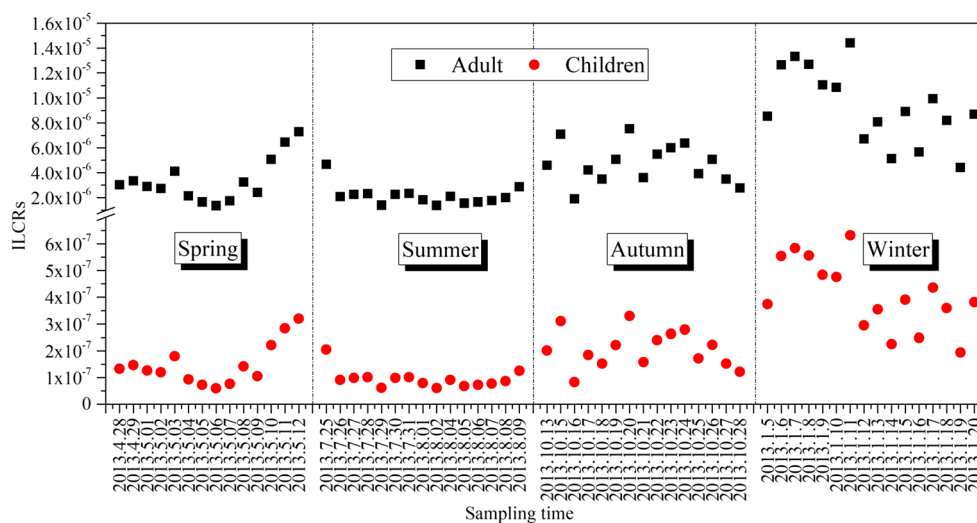
### Health risk assessments

Figure 4 shows the ILCRs during the entire sampling periods based on the method model mentioned in “Analysis of WTOC and WTN”. The values of BaP-eq concentration in spring, summer, autumn, and winter were in the range of 0.39 to 2.00 ng/m<sup>3</sup> (with an average of 0.93 ng/m<sup>3</sup>, same as below), 0.38 to 1.28 ng/m<sup>3</sup> (0.59 ng/m<sup>3</sup>), 0.52 to 2.06 ng/m<sup>3</sup> (1.29 ng/m<sup>3</sup>), and 1.21 to 3.95 ng/m<sup>3</sup> (2.55 ng/m<sup>3</sup>), respectively. The value of BaP-eq concentration in spring sampling periods were mostly lower than the standard provided by European Commission (1 ng/m<sup>3</sup>) (EU 2008); In summer, BaP-eq concentrations were higher than the standard provided by European Commission for only 1 day. In autumn, BaP-eq concentrations were higher than the standard provided by European Commission in vast majority of the sampling days. In all the sampling days in winter, BaP-eq concentrations were higher than the European Commission standard. The highest and lowest concentrations of BeP-eq appeared in winter and summer, respectively, and the highest/lowest (mean winter/summer) ratio was as high as 10.4.

Generally, an ILCR value less than or equal to  $1.0 \times 10^{-6}$  indicates non-significant or essentially negligible, and same as

the people some of the normal human activities for example diagnostic X-rays or radiation; the value of ILCRs between  $1.0 \times 10^{-6}$  and  $1.0 \times 10^{-4}$  stands for the potential risks to human health, whereas the value of ILCRs above  $1.0 \times 10^{-4}$  indicates higher risks (Chen and Liao 2006; EU 2008; WHO 2000). In this study, the total ILCRs for adult were in the range of  $1.36 \times 10^{-6}$  to  $7.29 \times 10^{-6}$  (mean  $3.39 \times 10^{-6}$ ),  $1.38 \times 10^{-6}$  to  $4.67 \times 10^{-6}$  (mean  $2.16 \times 10^{-6}$ ),  $1.89 \times 10^{-6}$  to  $7.53 \times 10^{-6}$  (mean  $4.70 \times 10^{-6}$ ), and  $4.42 \times 10^{-6}$  to  $1.44 \times 10^{-5}$  (mean  $9.33 \times 10^{-6}$ ) in spring, summer, autumn, and winter, respectively. The ILCRs in winter were mean four times higher than that of summer. As for the ILCRs for children, the values in spring, summer, autumn, and winter were in the scope of  $5.95 \times 10^{-8}$  to  $3.20 \times 10^{-7}$  (mean  $1.49 \times 10^{-7}$ ),  $6.05 \times 10^{-8}$  to  $2.05 \times 10^{-7}$  (mean  $9.46 \times 10^{-8}$ ),  $8.31 \times 10^{-8}$  to  $3.31 \times 10^{-7}$  (mean  $2.06 \times 10^{-7}$ ), and  $1.94 \times 10^{-7}$  to  $6.32 \times 10^{-7}$  (mean  $4.09 \times 10^{-7}$ ), respectively. The ILCRs in winter were mean an order of magnitude higher than that in summer. Moreover, the risks for adult were also mean an order of magnitude higher than that for children. The ILCRs decreased in the order of winter > autumn > summer > spring, and observed the same sequence as the concentration of PAHs in PM<sub>2.5</sub>, as shown in Fig. 6. In our study, the ILCRs during the entire sampling period were below the limit value of  $1.0 \times 10^{-4}$ , indicating that the carcinogenic risk for the residents who are exposed to the PM<sub>2.5</sub>-bound PAHs in our study area is essentially negligible but the detection rates of BaP, DBA, and BkF, which have no minimum safety limits during the entire sampling period, were up to 100%. The BaP-eq calculated by using these three rates accounted for 81% of the total BaP-eq, suggesting that the three carcinogenic PAH contaminants were the primary sources to the total BaP-eq. BkF and BaP have been used as a tracer for fossil fuels combustion and traffic emission (Rogge et al. 1993; Sadiktsis et al. 2012), DBA originated from high-temperature combustion (Sadiktsis et al. 2012). Therefore, we can safely infer that the pyrogenetic source and traffic emission play an important role on cancer risks.

**Fig. 6** The incremental lifetime cancer risks of PAHs



## Conclusions

This study described the concentrations of PM<sub>2.5</sub>-bound PAHs. The concentrations of PM<sub>2.5</sub> ranged from 6.96 to 260.06 µg/m<sup>3</sup> or mean 177.05 µg/m<sup>3</sup>. During the entire sampling period, only 38% of the days were superior to the 24-h limit value (75 µg/m<sup>3</sup>) of AAQs. The concentrations of PM<sub>2.5</sub> in autumn and winter exceeded the limit value. The total PAHs ranged from 1.51 to 44.51 ng/m<sup>3</sup> or mean 10.65 ng/m<sup>3</sup>. The highest and lowest concentrations of total PAHs appeared in winter and summer with averages of 22.56 and 4.03 ng/m<sup>3</sup>, respectively. The mass concentrations of PM<sub>2.5</sub> and PAHs manifested the same tendency: winter > autumn > spring > summer distribution. The 2-, 3-, 4-, 5-, and 6-ring PAHs accounted for 7.66, 9.92, 38.14, 20.71, and 23.56% of the total PAHs, respectively, and the four-, five-, and 6-ring PAHs were dominant in each sampling season.

The HMW-PAHs were negatively correlated with temperature and WTOC and significantly correlated with WTN. Source apportionment revealed that PM<sub>2.5</sub>-bound PAHs in Huangshi were mainly derived from pyrogenic source. PAHs were also mainly contributed by vehicle exhaust, coal combustion, and biomass burning. The ILCRs showed no potential carcinogenic risk from the PM<sub>2.5</sub>-bound BaP-eq, which represents total PAHs in the study area PM<sub>2.5</sub> at Huangshi. The averages of the total ILCRs for adults were  $3.39 \times 10^{-6}$ ,  $2.16 \times 10^{-6}$ ,  $4.70 \times 10^{-6}$ , and  $9.33 \times 10^{-6}$ , whereas the corresponding averages for children were  $3.39 \times 10^{-6}$ ,  $2.16 \times 10^{-6}$ ,  $4.70 \times 10^{-6}$ , and  $9.33 \times 10^{-6}$  in spring, summer, autumn, and winter, respectively. The ILCRs for adult and children decreased in the following order: winter > autumn > summer > spring. This pattern was the same as the concentration of PAHs. The risks in winter were the highest among the values observed in all seasons. The risks for adults were mean an order of magnitude higher than those for children.

**Acknowledgments** We gratefully thank Yong Zhang for collecting the sample.

**Funding information** The research was supported by the National Key Research and Development Program of China (2017YFC0212602), the Hubei Universities of Outstanding Young Scientific and Technological Innovation Team Plans (T201729), the Special Scientific Research Funds for National Basic Research Program of China (2013FY112700), the Outstanding Youth Science and Technology Innovation Team Projects of Hubei Polytechnic University (13xtz07), the Open Research Fund of Key Laboratory of Minal Environmental Pollution Control and Remediation in Hubei Province (201702).

## References

- Augusto S, Máguas C, Matos J, Pereira MJ, Branquinho C (2010) Lichens as an integrating tool for monitoring PAH atmospheric deposition: a comparison with soil, air and pine needles. *Environ Pollut* 158:483–489
- Bandowe BA, Meusel H, Huang RJ, Ho K, Cao J, Hoffmann T et al (2014) PM<sub>2.5</sub>-bound oxygenated PAHs, nitro-PAHs and parent-PAHs from the atmosphere of a Chinese megacity: seasonal variation, sources and cancer risk assessment. *Sci Total Environ* 473-474:77–87
- Bari MA, Baumbach G, Kuch B, Scheffknecht G (2010) Particle-phase concentrations of polycyclic aromatic hydrocarbons in ambient air of rural residential areas in southern Germany. *Air Qual Atmos Health* 3:103–116
- Beyer A, Wania F, Gouin T, Mackay D, Matthies M (2003) Temperature dependence of the characteristic travel distance. *Environ Sci Technol* 37:766–771
- Błaszczczyk E, Rogula-Kozłowska W, Klejnowski K, Fulara I, Mielżyńska-Svach D (2017) Polycyclic aromatic hydrocarbons bound to outdoor and indoor airborne particles (PM<sub>2.5</sub>) and their mutagenicity and carcinogenicity in Silesian kindergartens, Poland. *Air Qual Atmos Health* 10:389–400
- Callen MS, Iturmendi A, Lopez JM (2014) Source apportionment of atmospheric PM<sub>2.5</sub>-bound polycyclic aromatic hydrocarbons by a PMF receptor model. Assessment of potential risk for human health. *Environ Pollut* 195:167–177
- Chen F, Hu W, Zhong Q (2013) Emissions of particle-phase polycyclic aromatic hydrocarbons (PAHs) in the Fu Gui-shan Tunnel of Nanjing, China. *Atmos Res* 124:53–60
- Chen SC, Liao CM (2006) Health risk assessment on human exposed to environmental polycyclic aromatic hydrocarbons pollution sources. *Sci Total Environ* 366:112–123
- Chen Y, Li X, Zhu T, Han Y, Lv D (2017) PM<sub>2.5</sub>-bound PAHs in three indoor and one outdoor air in Beijing: concentration, source and health risk assessment. *Sci Total Environ* 586:255–264
- Correia AW, Pope CA, Dockery DW, Wang Y, Ezzati M, Dominici F (2013) Effect of air pollution control on life expectancy in the United States an analysis of 545 US counties for the period from 2000 to 2007. *Epidemiology* 24:23–31
- Decesari S, Facchini MC, Fuzzi S, Tagliavini E (2000) Characterization of water-soluble organic compounds in atmospheric aerosol: a new approach. *J Geophys Res-Atmos* 105:1481–1489
- EU (2008) Directive of the European Parliament and of the Council on Ambient Air Quality and Cleaner Air for Europe. European Union. <http://ec.europa.eu/environment/air/quality/standards.htm>. Accessed 8 January 2018
- Fraser MP, Cass GR, Simoneit BR, Rasmussen R (1997) Air quality model evaluation data for organics. 4. C<sub>2</sub>-C<sub>36</sub> non-aromatic hydrocarbons. *Environ Sci Technol* 31:2356–2367
- GB3095-2012 (2012) National Ambient Air Quality Standards in China. Ministry of Environmental Protection and General Administration of Quality Supervision, Inspection and Quarantine of the People's Republic of China. [http://kjs.mep.gov.cn/hjbhbz/bzwb/dqjhbh/dqhjzlbz/201203/t20120302\\_224165.shtml](http://kjs.mep.gov.cn/hjbhbz/bzwb/dqjhbh/dqhjzlbz/201203/t20120302_224165.shtml). Accessed 8 January 2018
- Geng NB, Wang J, Xu YF, Zhang WD, Chen C, Zhang RQ (2013) PM<sub>2.5</sub> in an industrial district of Zhengzhou, China: chemical composition and source apportionment. *Particuology* 11:99–109
- Günther T, Dornberger U, Fritsche W (1996) Effects of ryegrass on biodegradation of hydrocarbons in soil. *Chemosphere* 33:203–215
- Hu TP, Zhang JQ, Ye C, Zhang L, Xing XL, Zhang Y et al (2017) Status, source and health risk assessment of polycyclic aromatic hydrocarbons (PAHs) in soil from the water-level-fluctuation zone of the three gorges reservoir, China. *J Geochem Explor* 172:20–28
- Karar K, Gupta AK (2006) Seasonal variations and chemical characterization of ambient PM<sub>10</sub> at residential and industrial sites of an Urban region of Kolkata (Calcutta), India. *Atmos Res* 81:36–53
- Khalili NR, Scheff PA, Holsen TM (1995) PAH source fingerprints for coke ovens, diesel and, gasoline engines, highway tunnels, and wood combustion emissions. *Atmos Environ* 29:533–542
- Khan MF, Latif MT, Lim CH, Amil N, Jaafar SA, Dominick D, Mohd Nadzir MS, Sahani M, Tahir NM (2015) Seasonal effect and source apportionment of polycyclic aromatic hydrocarbons in PM<sub>2.5</sub>. *Atmos Environ* 106:178–190

- Kim KH, Kabir E, Kabir S (2015) A review on the human health impact of airborne particulate matter. *Environ Int* 74:136–143
- Lai IC, Lee CL, Zeng KY, Huang HC (2011) Seasonal variation of atmospheric polycyclic aromatic hydrocarbons along the Kaohsiung coast. *J Environ Manag* 92:2029–2037
- Larsen RK, Baker JE (2003) Source apportionment of polycyclic aromatic hydrocarbons in the urban atmosphere: a comparison of three methods. *Environ Sci Technol* 37:1873–1881
- Lee JY, Shin HJ, Bae SY, Kim YP, Kang C-H (2008) Seasonal variation of particle size distributions of PAHs at Seoul, Korea. *Air Qual Atmos Health* 1:57–68
- Leitte AM, Schlink U, Herbarth O, Wiedensohler A, Pan XC, Hu M et al (2011) Size-segregated particle number concentrations and respiratory emergency room visits in Beijing, China. *Environ Health Perspect* 119:508–513
- Li X, Kong S, Yin Y, Li L, Yuan L, Li Q, Xiao H, Chen K (2016) Polycyclic aromatic hydrocarbons (PAHs) in atmospheric PM<sub>2.5</sub> around 2013 Asian Youth Games period in Nanjing. *Atmos Res* 174-175:85–96
- Liu J, Man R, Ma S, Li J, Wu Q, Peng J (2015) Atmospheric levels and health risk of polycyclic aromatic hydrocarbons (PAHs) bound to PM<sub>2.5</sub> in Guangzhou, China. *Mar Pollut Bull* 100:134–143
- Nisbet ICT, Lagoy PK (1992) Toxic equivalency factors (Tefs) for polycyclic aromatic-hydrocarbons (Pahs). *Regul Toxicol Pharmacol* 16: 290–300
- Niu ZC, Zhou WJ, Wu SG, Cheng P, Lu XF, Xiong XH, Du H, Fu Y, Wang G (2016) Atmospheric fossil fuel CO<sub>2</sub> traced by Delta C-14 in Beijing and Xiamen, China: temporal variations, inland/coastal differences and influencing factors. *Environ Sci Technol* 50:5474–5480
- Novakov T, Penner JE (1993) Large contribution of organic aerosols to cloud-condensation-nuclei concentrations. *Nature* 365:823–826
- Panther BC, Hooper MA, Tapper NJ (1999) A comparison of air particulate matter and associated polycyclic aromatic hydrocarbons in some tropical and temperate urban environments. *Atmos Environ* 33:4087–4099
- Rogge WF, Hildemann LM, Mazurek MA, Cass GR, Simoneit BR (1993) Sources of fine organic aerosol. 2. Nuncatalyst and catalyst-equipped automobiles and heavy-duty diesel trucks. *Environ Sci Technol* 27:636–651
- Sadiktsis I, Bergvall C, Johansson C, Westerholm R (2012) Automobile tires: a potential source of highly carcinogenic dibenzopyrenes to the environment. *Environ Sci Technol* 46:3326–3334
- Shulman ML, Jacobson MC, Carlson RJ, Synovec RE, Young TE (1996) Dissolution behavior and surface tension effects of organic compounds in nucleating cloud droplets. *Geophys Res Lett* 23:277–280
- Tao J, Zhang LM, Engling G, Zhang RJ, Yang YH, Cao JJ, Zhu C, Wang Q, Luo L (2013) Chemical composition of PM<sub>2.5</sub> in an urban environment in Chengdu, China: importance of springtime dust storms and biomass burning. *Atmos Res* 122:270–283
- Wania F, Mackay D (1995) A global distribution model for persistent organic-chemicals. *Sci Total Environ* 160-61:211–232
- Wania F, Mackay D (1996) Tracking the distribution of persistent organic pollutants. *Environ Sci Technol* 30:A390–A396
- WHO (2000) Air quality guidelines for Europe, 2nd ed. WHO Regional Office for Europe, Copenhagen. <http://www.who.int/iris/handle/10665/107335>. Accessed 8 January 2018
- WHO (2005) Air quality guidelines global update: particulate matter, ozone, nitrogen dioxide and sulfur dioxide. WHO Regional Office for Europe, Copenhagen. <http://www.who.int/iris/handle/10665/107823>. Accessed 8 January 2018
- Xing XL, Qi SH, Zhang JQ, Wu CX, Zhang Y, Yang D, Odhiambo JO (2011) Spatial distribution and source diagnosis of polycyclic aromatic hydrocarbons in soils from Chengdu Economic Region, Sichuan Province, western China. *J Geochem Explor* 110:146–154
- Xing XL, Zhang Y, Yang D, Zhang JQ, Chen W, Wu CX, Liu H, Qi S (2016) Spatio-temporal variations and influencing factors of polycyclic aromatic hydrocarbons in atmospheric bulk deposition along a plain-mountain transect in western China. *Atmos Environ* 139: 131–138
- Xu HM, Ho SSH, Gao ML, Cao JJ, Guinot B, Ho KF, Long X, Wang J, Shen Z, Liu S, Zheng C, Zhang Q (2016) Microscale spatial distribution and health assessment of PM<sub>2.5</sub>-bound polycyclic aromatic hydrocarbons (PAHs) at nine communities in Xi'an, China. *Environ Pollut* 218:1065–1073
- Yang GH, Wang Y, Zeng YX, Gao GF, Liang XF, Zhou MG, Wan X, Yu S, Jiang Y, Naghavi M, Vos T, Wang H, Lopez AD, Murray CJL (2013) Rapid health transition in China, 1990–2010: findings from the global burden of disease study 2010. *Lancet* 381:1987–2015
- Yang H, Li QF, Yu JZ (2003) Comparison of two methods for the determination of water-soluble organic carbon in atmospheric particles. *Atmos Environ* 37:865–870
- Yunker MB, Macdonald RW, Vingarzan R, Mitchell RH, Goyette D, Sylvestre S (2002) PAHs in the Fraser River basin: a critical appraisal of PAH ratios as indicators of PAH source and composition. *Org Geochem* 33:489–515
- Zhang F, Wang ZW, Cheng HR, Lv XP, Gong W, Wang XM, Zhang G (2015a) Seasonal variations and chemical characteristics of PM<sub>2.5</sub> in Wuhan, central China. *Sci Total Environ* 518-519:97–105
- Zhang JQ, Qu CK, Qi SH, Cao JJ, Zhan CL, Xing XL, Xiao Y, Zheng J, Xiao W (2015b) Polycyclic aromatic hydrocarbons (PAHs) in atmospheric dustfall from the industrial corridor in Hubei Province, Central China. *Environ Geochem Health* 37:891–903
- Zhang JQ, Zhan CL, Liu HX, Liu T, Yao RZ, Hu TP, Xiao W, Xing X, Xu H, Cao J (2016) Characterization of polycyclic aromatic hydrocarbons (PAHs), Iron and black carbon within street dust from a steel industrial city, central China. *Aerosol Air Qual Res* 16:2452–2461
- Zhang YX, Tao S (2008) Seasonal variation of polycyclic aromatic hydrocarbons (PAHs) emissions in China. *Environ Pollut* 156:657–663